forum acusticum 2026
8-12 September · Graz, Austria

AUTONOMOUS AIRCRAFT NOISE RECORDING: DEVELOPING DATASETS FOR MACHINE LEARNING

Gary Isherwood[1], Paul Newbury[1]

[1] *Department of Informatics, University of Sussex, United Kingdom*

This paper is a revised version of the authors' submitted manuscript that was peer-reviewed by at least two anonymous reviewers.

Abstract

The advancement of deep learning in environmental acoustics is hindered by a lack of high-fidelity, labelled datasets. While aircraft noise is a major environmental concern, collecting annotated data at scale remains a logistical hurdle; attended measurements lack volume and permanent monitors lack geographic diversity. This paper presents an autonomous aircraft noise recording station that integrates a noise monitoring terminal with a custom solar-power subsystem and ADS-B (Automatic Dependent Surveillance–Broadcast) receiver. This architecture enables automatic alignment of acoustic events with flight telemetry, including aircraft type, location and altitude in order to reduce manual annotation effort. In this paper, an "AI-ready" acoustic event refers to a recorded aircraft-noise segment paired with metadata describing the associated aircraft identifier, aircraft category where available, timestamped position, altitude, and derived source–receiver geometry, together with environmental flags indicating potentially compromised measurement periods.

Keywords: *aircraft noise, unattended monitoring, acoustic measurement, data acquisition, machine learning datasets*

1. Introduction

Aircraft noise remains one of the most significant sources of environmental noise pollution, with documented adverse effects on public health, sleep quality, and annoyance in communities surrounding airports [1], [2], [3]. As air traffic volume expands [4], the need for accurate, automated noise monitoring and classification has never been more critical. Recent advancements in machine learning (ML), particularly in deep neural networks, offer promising new avenues for analysing complex acoustic environments [5], [6]. However, the efficacy of these data-driven models is fundamentally limited by the quality and quantity of available training data [7], [8].

1.1. The labelling bottleneck

Training robust supervised learning models requires thousands of diverse examples to prevent overfitting [9]. In the context of aircraft noise, this presents a unique challenge. While raw audio is relatively easy to record, "ground truth" labels confirming that a specific sound event is indeed an aircraft, and identifying its type or trajectory are difficult to generate at scale [10], [11]. Traditional datasets often rely on manual annotation, which is labour-intensive and prone to human error [12], [13]. Alternative approaches that attempt to retrospectively match audio recordings with data from commercial flight tracking APIs often suffer from rate limits, licensing constraints, or significant temporal misalignment between the API's reported time and the local recording clock [14], [15].

1.2. The Need for Autonomous Data Collection

To satisfy the needs of modern ML architectures [7], [10], a shift is required from short-term, attended measurements to long-term, autonomous field campaigns. An ideal system should be capable of operating unattended for weeks in diverse locations, capturing not just the noise of the airport runway, but the propagation of noise in rural and suburban environments where low signal-to-noise ratios challenge current detection algorithms [16].

This paper describes the design and deployment of an autonomous recording station developed to meet these requirements. The system addresses three primary challenges in field data collection:

1. **Energy Autonomy:** Managing power budgets to allow extended operation without mains electricity, even during winter months.

2. **Data Integrity:** Ensuring reliable synchronisation between acoustic capture and flight telemetry (ADS-B) to allow for automated labelling.

Corresponding author: *g.isherwood@sussex.ac.uk.*

3. **Environmental Resilience:** Maintaining measurement accuracy in variable weather conditions typical of the UK climate.

By addressing these hurdles, this paper demonstrates a repeatable methodology for curating 'AI-ready' datasets. The resulting field deployment configuration is shown in Fig. 1.

Figure 1: Field deployment configuration at the Penshurst site: the IMS NoiseGuard terminal and EcoFlow auxiliary power station within water-resistant enclosures, a 160 W solar array, and a Class 2 microphone tripod-mounted at 1.5 m over grass.

2. Requirements & Field Challenges

The system supports long-duration aircraft noise recording for data-driven analysis, emphasising repeatability, robustness and data quality across deployments.

2.1. Operational Requirements

Deployments necessitate unattended operation for extended multi-month periods, frequently at locations without reliable mains electricity. The system therefore requires an off-grid power source and local energy storage capable of sustaining continuous operation without introducing persistent acoustic emissions. Conventional fuel-based generators are unsuitable due to their continuous noise output and the risk of contaminating acoustic measurements [17], [18].
Outdoor operation additionally requires procedures to mitigate precipitation-related measurement artefacts. The system should therefore incorporate a mechanism to identify and exclude rainfall-affected periods from the dataset [19], [20].

2.2. Acoustic Requirements

From an acoustic standpoint, the system should reliably capture aircraft flyover events with sufficient signal-to-noise ratio to support both conventional acoustic metrics and downstream machine learning analysis.

Extended outdoor operation introduces measurement artefacts not typically encountered in short-term surveys. Wind-induced self-noise, precipitation impact on the microphone assembly, and vibration from mounting structures are recognised sources of degradation in environmental noise recordings [18], [21]. The acoustic front-end therefore requires appropriate wind and weather protection, while acknowledging that foam windscreens alone may exhibit reduced transparency under strong wind or when saturated, as noted in environmental noise measurement protocols [17].

Aircraft-noise measurement practice is strongly shaped by standardised procedures for certification and environmental assessment. For example, ICAO Annex 16, Volume I specifies aircraft noise certification procedures and associated noise measurement and evaluation methods, including requirements that are beyond the scope of the present autonomous dataset-acquisition study [22].The present work is not proposed as a certification or compliance measurement campaign. Instead, it addresses a complementary requirement: a repeatable autonomous field architecture for collecting aircraft-noise recordings, ADS-B-derived trajectory metadata and environmental quality flags under realistic unattended deployment conditions.

2.3. Data and Metadata Requirements

Required fields include Coordinated Universal Time (UTC) timestamps, aircraft hexadecimal identifiers derived from transponder-based tracking [14], aircraft category information where available, geographic position, ground speed, barometric and geometric altitude, flight track angle, and flight identification codes. Acoustic descriptors shall include equivalent continuous sound pressure level (e.g., $L_{Aeq,1s}$) and sound exposure level (SEL) in accordance with standard environmental noise metrics [17].

2.4. Environmental Context and Data Validation

Continuous monitoring of local meteorological conditions identifies periods where the microphone's physical properties or the propagation path may be compromised.

Relative humidity and temperature require logging at an interval sufficient to capture sustained atmospheric trends without exceeding energy or storage constraints, flagging potential moisture-induced sensitivity shifts in the acoustic front-end. Rainfall should be flagged to allow optional exclusion of "wet" recordings, where impact noise on the microphone assembly would contaminate the aircraft's spectral signature.

3. System Architecture

The recording station comprises three primary modules: the acoustic recording terminal, a solar-powered energy subsystem and the environmental enclosures. This architecture is designed for rapid deployment and long-term autonomy in remote field conditions.

3.1. Recording and Data Acquisition

The system utilises an IMS Noise Guard IoT Portable (Class 2) terminal for synchronised acoustic and telemetry capture. Unlike standard continuous monitors, the terminal performs event-based recording with ADS-B telemetry alignment. As recorded in the system logs, each event is programmatically defined by a discrete start and end time, corresponding to the aircraft's presence within the receiver's detection radius. For each detected event, the terminal generates a raw audio recording alongside a structured metadata record (e.g., aircraft hexadecimal identifier and flight identification where available). Acoustic metrics including $L_{Aeq,1s}$ are logged over the event duration and Sound Exposure Level (SEL) is computed. Data are transmitted via an integrated 4G modem to a cloud portal, with local buffering to mitigate temporary network outages. Audio was recorded in mono at 48 kHz and stored as 48 kbps MPEG-1 Audio Layer III (MP3). Usable high-frequency content is constrained by the lossy encoding and low bitrate. No high-pass filter was applied during post-processing; the lower frequency limit is therefore set by the terminal response, which extends down to 20 Hz in accordance with IEC 61672-1 Class 2 requirements.

3.2. Power Subsystem and Energy Budget

To provide near-silent, off-grid operation, the terminal's internal LiPo battery is supported by a 512 Wh EcoFlow RIVER 2 Max power station and a 160 W solar array. The system's power requirements were characterised at 10°C, showing a mean draw of 6.5 W. Although the setup utilises a 240 V AC adapter, introducing an estimated 15% conversion loss through the inverter, the energy budget indicates that the system remains energy-positive in most conditions. The theoretical buffer runtime (T_{buff}) without solar input is:

$$T_{buff} = \frac{C_{bat} \times \eta}{P_{load}} \approx 67 \text{ hours} \tag{1}$$

where C_{bat} is the auxiliary battery capacity, η is the inverter efficiency (0.85), and P_{load} is the mean draw. To support year-round autonomy in the UK climate, a physical timer-switch restricts monitoring to a 5-hour peak traffic window (11:00–16:00) during winter, reducing the projected daily consumption to approximately 52 Wh.

Table 1 summarises the two seasonal operating configurations. The summer configuration was checked against field observations during a two-week trial, reported in Section 5.1. The winter configuration has been implemented in hardware but has not yet been assessed over a formal trial period; the winter values in Table 1 should therefore be interpreted as energy-budget projections rather than field-validated performance.

3.3. Enclosure and Environmental Protection

While the NoiseGuard terminal is weather-resistant, its AC power cables and the auxiliary EcoFlow power station are not IP-rated. To ensure weatherproofing, both the terminal and the power supply are housed within secondary water-resistant enclosures. These housings are linked via waterproof conduit and IP-rated cable glands to protect vulnerable connections from moisture.

To prevent heat accumulation, particularly during the charging cycles of the power station, custom 3D printed passive vent inserts were integrated into the enclosures. This passive cooling approach was prioritised over active fans to eliminate potential acoustic contamination of the recordings. During autumn and winter deployments in the UK, these measures prevented water ingress and internal condensation despite sustained high humidity and rainfall.

Table 1: Seasonal operating configurations. Summer values are consistent with a two-week field trial (Section 5.1); winter values are energy-budget projections not yet validated in the field.

Parameter	Value (Winter/Summer)
Duty Cycle	11:00–16:00 / Constant
Daily Energy Draw	∼52 Wh / ∼156 Wh
Solar Yield	80–120 Wh / 600–800 Wh
State of Charge	Net Positive / Surplus
Buffer (No Sun)	∼13 Days / ∼2.7 Days

3.4. Site Selection

Deployments were conducted at two contrasting locations:

- **Brighton:** Initial trials at Brighton, UK (50.8553° N, 0.0965° W) targeted high-altitude arrivals and departures above approximately 10,000 ft. At these source–receiver distances, aircraft Sound Exposure Level (SEL) frequently fell close to or below the local ambient noise floor. This environment was therefore useful as a stress test for trigger sensitivity and energy autonomy but produced relatively few recordings suitable for detailed spectral analysis.

- **Penshurst:** A second site was selected near Gatwick Airport arrival paths at Penshurst Place, Kent, UK (51.1771° N, 0.1862° E). This site provided higher-SNR aircraft signatures, with a modal aircraft altitude of approximately 4,000 ft [23]. By capturing events in a rural setting rather than at the airport perimeter, the deployment provides recordings with a different propagation distance and background soundscape from near-runway monitoring, while retaining sufficient signal quality for event segmentation and preliminary spectral analysis.

Future deployments should combine sites near lower-altitude flight paths with more distant community-monitoring locations to balance signal quality against geographic diversity.

3.5. Physical Setup

Microphones were tripod-mounted at 1.5 m height, adhering to ISO 1996-2:2017 standards for environmental noise assessment. A custom 3D-printed mount was developed to secure the ADS-B receiver and the Lascar EL-USB-2-LCD temperature/humidity logger directly to the tripod assembly.
The humidity sensor was set to a 30-minute sampling interval, providing approximately 11 months of internal memory capacity. Similarly, the precipitation sensor utilised an internal storage buffer capable of holding 8 months of data.
All recordings took place over soft ground (grass). Ground effect phase cancellation, typically affecting mid-range frequencies, was intentionally left uncorrected. This approach preserves the realistic acoustic signature as perceived by a ground-based observer, providing the ML model with a more authentic representation of real-world immission levels [24].

3.6. Calibration and Quality Control

The Noise Guard IoT Portable terminal was verified for acoustic accuracy by the manufacturer prior to the initial deployment phase. No independent laboratory calibration was performed by the authors during this pilot study; however, the unit was specified by the manufacturer as meeting Class 2 requirements under IEC 61672-1 for environmental noise monitoring.
Environmental quality control is applied in post-processing using the ICAO Annex 16 meteorological test window as a reference rather than as a claim of certification compliance. Temperature and relative humidity were logged using a Lascar EL-USB-2-LCD logger, while precipitation was recorded using a separate rain sensor. Recordings were excluded when their timestamps overlapped with any rain-sensor indication of precipitation or residual wetness. Temperature and relative-humidity records were screened against the Annex 16 limits of −10–35 °C and 20–95%, respectively [22]. Recordings outside these ranges are flagged for exclusion during dataset preparation. Wind speed and the full set of Annex 16 propagation-path meteorological requirements were not measured, so full Annex 16 test-window compliance cannot be claimed. Campaign-level signal stability was not assessed in this pilot study. Future deployments will include early–late comparisons of SEL and spectral noise-floor estimates as part of the quality-control pipeline.

4. Data Handling & Integrity

The following protocols govern data synchronisation and feature extraction.

4.1. Transmission and Temporal Alignment

Acoustic events and ADS-B telemetry are recorded using Coordinated Universal Time (UTC) timestamps at the point of acquisition, supporting sub-second alignment without relying on post-hoc matching to external flight-tracking APIs [15]. The associated aircraft position should therefore be interpreted as ADS-B source-time geometry. The acoustic waveform is received at the microphone after a propagation delay that varies with source–receiver distance, so the present dataset is not fully corrected to retarded, receiver-time geometry. Propagation-delay correction is identified as a future improvement.

4.2. Data Structure and Derived Features

The raw data is logged in a structured CSV format containing geodetic coordinates (Latitude ϕ, Longitude λ) and altitude (h) derived from the ADS-B stream. Since received aircraft noise is strongly influenced by source–receiver distance, the Slant Distance (r) is computed post-hoc for every timestamp. This is derived using the Haversine formula [25] to determine the ground arc distance (d_{ground}), combined with the relative altitude difference:

$$r = \sqrt{d_{ground}^2 + (h_{plane} - h_{mic})^2} \tag{2}$$

Slant distance is included as a first-order source–receiver geometry descriptor, providing a compact estimate of propagation distance at each timestamp. It is not intended to fully describe aircraft-noise radiation or certification-relevant measurement geometry. Parameters such as elevation angle, aircraft attitude, engine operating state, atmospheric conditions and certification-style trajectory descriptors would be required for a more complete aeroacoustic analysis.

5. Preliminary Results

5.1. System Autonomy

As an operational check of the summer configuration, the power system was observed over a two-week trial beginning on 15 June 2025, with the terminal recording continuously. During this period, the battery state of charge (SoC) remained between 64% and 100%, and no manual recharging was required, including across consecutive overcast days. These observations are consistent with the summer energy budget in Table 1 and indicate that the 160 W array comfortably replenishes the ∼156 Wh daily draw under UK summer conditions.
These results are an operational feasibility check rather than a year-round energy audit; validating the projected winter energy balance in Table 1 is a priority for the next deployment.

5.2. Acoustic Capture and Alignment

Initial trials at the Penshurst site produced recordings in which aircraft events were clearly distinguishable from the background. The spectrogram of a representative Airbus A320 arrival (Fig. 2) shows broadband energy rising toward closest approach before decreasing as the aircraft recedes, with most event energy concentrated below 2 kHz. Faint harmonic-like structures are visible near the event peak but the present analysis does not assign them to a specific engine order or blade-passing frequency as they may be affected by source motion, ground reflection, atmospheric propagation and MP3 compression.
Event-level SEL values and $L_{Aeq,1s}$ traces were gener-

ated for each detected event; for the flyover in Fig. 2, the $L_{Aeq,1s}$ peak exceeded the background level (L_{90}) by approximately 24 dB. Across the Penshurst deployment as a whole, detected events had a median event SEL of 69.7 dB(A) (N = 22,158 events) and a median peak $L_{Aeq,1s}$ of 58.3 dB(A) (interquartile range 53.9–62.2 dB(A), computed over the 17,621 events with complete second-by-second level traces), indicating that captured flyovers typically stand well above the rural ambient. As the site lies under a busy arrival corridor, approximately 86% of event windows overlapped in time with at least one other detected aircraft, so per-event levels may include contributions from more than one source. The per-second trajectory metadata allows such events to be identified and, where required, excluded or re-windowed around each aircraft's closest approach during dataset preparation.

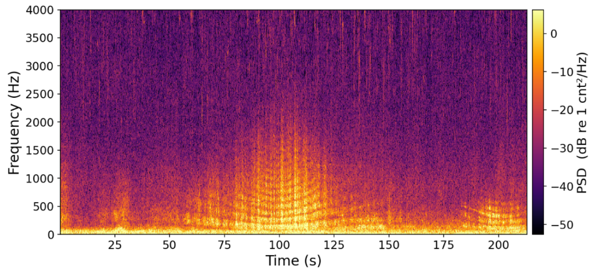

Figure 2: Spectrogram of a representative Airbus A320 arrival at the Penshurst site ($h \approx$ 4,540 ft, $r \approx$ 1,450 m at closest approach, ADS-B source-time geometry). Computed from 48 kHz audio (4096-point FFT, Hann window, 512-sample hop); levels are PSD in dB relative to digital counts (uncalibrated).

6. Recommendations for AI Datasets

Based on the development of this autonomous station, this paper proposes several recommendations for the creation of environmental acoustics datasets intended for machine learning.

6.1. Defining the Data Acquisition Boundary

This paper focuses strictly on the acquisition and synchronisation phase of dataset creation. Temporal segmentation (cropping of event windows) and spectral denoising are intentionally excluded from this hardware-focused methodology; providing raw data allows researchers to apply their own windowing and augmentation strategies.

6.2. Geographic Diversity for Dataset Design

Recordings collected away from airport perimeters may expose models to lower-SNR events, longer propagation paths and more varied background soundscapes than near-runway datasets, reducing over-reliance on high-amplitude near-field signatures. The present work does not prove model generalisability, but identifies geographic and acoustic diversity as a design requirement for future aircraft-noise datasets. In addition, local ADS-B reception provides aircraft identifiers and trajectory metadata at the point of acquisition, reducing reliance on post-hoc matching with external flight-tracking services.

6.3. Feature Engineering for ML

This paper recommends that datasets produced using this methodology include derived spatial features, such as the Slant Distance (r) calculated in Section 4.2. Providing this feature alongside the audio may reduce the need for a model to infer basic three-dimensional geometry from raw coordinates alone. However, slant distance should be treated as a first-order descriptor rather than a complete representation of aircraft-noise propagation, with source directivity, aircraft operating state and atmospheric effects left for future work.

Acknowledgments

The authors acknowledge EPSRC and the University of Sussex for support, IMS Measurement Systems for technical assistance, and Penshurst Place for site access.

References

[1] World Health Organization, *Environmental Noise Guidelines for the European Region*. Copenhagen, Denmark: WHO Regional Office for Europe, 2018, `https://www.who.int/europe/publications/i/item/9789289053563`.

[2] M. Basner and S. McGuire, "Who environmental noise guidelines for the european region: A systematic review on environmental noise and effects on sleep," *International Journal of Environmental Research and Public Health*, vol. 15, no. 3, p. 519, 2018.

[3] R. Guski, D. Schreckenberg, and R. Schuemer, "Who environmental noise guidelines for the european region: A systematic review on environmental noise and annoyance," *International Journal of Environmental Research and Public Health*, vol. 14, no. 12, p. 1539, 2017. DOI: `10.3390/ijerph14121539`.

[4] EUROCONTROL, "Eurocontrol forecast update 2025–2031," EUROCONTROL, Tech. Rep., Oct. 2025, Accessed: 2026-01-28. [Online]. Available: `https://www.eurocontrol.int/publication/eurocontrol-forecast-update-2025-2031`.

[5] J. Abeßer, "A review of deep learning based methods for acoustic scene classification," *Applied Sciences*, vol. 10, no. 6, p. 2020, 2020, Accessed: 2026-01-28. DOI: `10.3390/app10062020`. [Online]. Available: `https://www.mdpi.com/2076-3417/10/6/2020`.

[6] S. Hershey et al., "Cnn architectures for large-scale audio classification," in *ICASSP*, 2017.

[7] Y. LeCun, Y. Bengio, and G. Hinton, “Deep learning,” *Nature*, vol. 521, no. 7553, pp. 436–444, 2015, Accessed: 2026-01-28. DOI: 10.1038/nature14539. [Online]. Available: https://www.nature.com/articles/nature14539.

[8] J. Salamon and J. P. Bello, “Deep convolutional neural networks and data augmentation for environmental sound classification,” *IEEE Signal Processing Letters*, vol. 24, no. 3, pp. 279–283, 2017, Accessed: 2026-01-28. DOI: 10.1109/LSP.2017.2657381. [Online]. Available: https://ieeexplore.ieee.org/document/7878751.

[9] I. Goodfellow, Y. Bengio, and A. Courville, *Deep Learning*. MIT Press, 2016, Accessed: 2026-01-28. [Online]. Available: https://www.deeplearningbook.org/.

[10] B. Downward and J. Nordby, *Aerosonicdb (ypad-0523): Labelled audio dataset for acoustic detection and classification of aircraft*, Accessed: 2026-01-28, Zenodo, 2023. DOI: 10.5281/zenodo.8004081. [Online]. Available: https://zenodo.org/records/8004081.

[11] X. Zhang et al., “Exploring acoustic characteristics of different aircraft types using ads-b–based labeling,” *Journal of the Acoustical Society of America*, vol. 153, no. 5, p. 3138, 2023, Accessed: 2026-01-28. DOI: 10.1121/10.0019594. [Online]. Available: https://pubs.aip.org/asa/jasa/article/153/5/3138/2893306/Exploring-acoustic-characteristics-of-different.

[12] C. G. Northcutt, L. Jiang, and I. L. Chuang, “Confident learning: Estimating uncertainty in dataset labels,” *Journal of Artificial Intelligence Research*, vol. 70, pp. 1373–1411, 2021, Accessed: 2026-01-28. DOI: 10.1613/jair.1.12125. [Online]. Available: https://www.jair.org/index.php/jair/article/view/12125.

[13] R. Snow, B. O’Connor, D. Jurafsky, and A. Ng, “Cheap and fast—but is it good? evaluating non-expert annotations for natural language tasks,” in *Proceedings of EMNLP*, Accessed: 2026-01-28, 2008, pp. 254–263. [Online]. Available: https://aclanthology.org/D08-1027/.

[14] M. Schäfer, M. Strohmeier, V. Lenders, I. Martinovic, and M. Wilhelm, “Bringing up opensky: A large-scale ads-b sensor network for research,” in *Proceedings of the 13th International Symposium on Information Processing in Sensor Networks (IPSN)*, Accessed: 2026-01-28, 2014, pp. 83–94. DOI: 10.1109/IPSN.2014.6846743. [Online]. Available: https://ieeexplore.ieee.org/document/6846743.

[15] K. Jansen, “Possibilities and limitations using flightradar24, ads-b and mode s data for aircraft performance analysis,” Hamburg University of Applied Sciences (HAW Hamburg), Project Report, 2020. [Online]. Available: https://www.fzt.haw-hamburg.de/pers/Scholz/arbeiten/TextJansen.pdf.

[16] D. K. Wilson, C. L. Pettit, V. E. Ostashev, and S. N. Vecherin, “Description and quantification of uncertainty in outdoor sound propagation calculations,” *Journal of the Acoustical Society of America*, vol. 136, no. 3, pp. 1013–1028, 2014, Accessed: 2026-01-28. DOI: 10.1121/1.4890644. [Online]. Available: https://pubmed.ncbi.nlm.nih.gov/25190377/.

[17] *ISO 1996-2:2017 acoustics – description, measurement and assessment of environmental noise – part 2: Determination of environmental noise levels*, International Organization for Standardization, 2017.

[18] R. Raspet, J. Yu, and J. Webster, “Low frequency wind noise contributions in measurement microphones,” *The Journal of the Acoustical Society of America*, 2008, Accessed: 2026-01-28. DOI: 10.1121/1.2832329. [Online]. Available: https://pubmed.ncbi.nlm.nih.gov/18345815/.

[19] C. Ribeiro, D. Ecotière, P. Cellard, and C. Rosin, “Uncertainties of the frequency response of wet microphone windscreens,” *Applied Acoustics*, vol. 78, pp. 11–18, 2014. DOI: 10.1016/j.apacoust.2013.10.005.

[20] R. A. Wright and G. Goulamhoussen, “Effects of weather on outdoor microphone windshields,” in *Institute of Acoustics Conference Proceedings*, 2011.

[21] O. Eldwaik and F. F. Li, “Mitigating wind induced noise in outdoor microphone signals using a singular spectral subspace method,” *Technologies*, vol. 6, no. 1, p. 19, 2018, Accessed: 2026-01-28. DOI: 10.3390/technologies6010019. [Online]. Available: https://www.mdpi.com/2227-7080/6/1/19.

[22] International Civil Aviation Organization, *Annex 16 to the Convention on International Civil Aviation: Environmental Protection, Volume I—Aircraft Noise*, 8th ed. Montreal: International Civil Aviation Organization, 2017. Accessed: Jul. 7, 2026.

[23] Gatwick Airport. “How high are flights in my area? – Gatwick Insightful,” Accessed: Feb. 12, 2026. [Online]. Available: https://aircraftnoise.gatwickairport.com/2020/07/31/how-high-are-flights-in-my-area/.

[24] K. Attenborough, “Review of ground effects in outdoor propagation,” *Journal of Sound and Vibration*, vol. 124, no. 3, pp. 401–454, 1988.

[25] R. W. Sinnott, “Virtues of the haversine,” *Sky and Telescope*, vol. 68, no. 2, p. 158, 1984.